# Integrating the coproduction of cellulose nanofibers and biobutanol from eucalyptus pulp using an environmentally friendly process

Florencia Cebreiros[a,*], Gustavo Sánchez[b], Mario Daniel Ferrari[a], Claudia Lareo[a]

[a]Departamento de Bioingeniería, Facultad de Ingeniería, Universidad de la República, Julio Herrera y Reissig 565, CP 11300, Montevideo, Uruguay.

[b]Departamento Ingeniería de Materiales y Minas, Facultad de Ingeniería, Universidad de la República, Julio Herrera y Reissig 565, CP 11300, Montevideo, Uruguay.

[*]Corresponding author. Tel.: +598 2714 2714 int 18118

E-mail address: fcebreiros@fing.edu.uy

## ABSTRACT

The combination of enzyme-mediated pretreatment with mechanical fibrillation has become an environmentally friendly and low-energy strategy to extract cellulose nanomaterials (CNM) from lignocellulosic biomass. The use of hydrolytic enzymes to produce CNM allows the coproduction of sugars that can be further converted to biofuels and/or value-added products. This work evaluated the integration of biobutanol production via fermentation of sugars released at high solid concentration with the biochemical platform of cellulose nanofibers (CNF) production. Cellulose fibers were partially hydrolyzed at low enzyme loadings (5 FPU/$g_{solid}$) and high solid concentrations (4-16%) obtaining a separate sugar stream (50 g/L), which was completely converted to biobutanol and coproducts (up to 15 g/L) by *Clostridium beijerinckii* strains. The cellulosic residue was mechanically defibrillated by ball milling to produce CNF (4-14 nm width, 220-230 aspect ratio). The enzyme fractionation represents a promising strategy to integrate the coproduction of CNF and biobutanol from cellulosic pulp.

**Keywords:** biobutanol, cellulose nanofibers, coproduction, *Clostridium*, ball milling

## 1. Introduction

In modern biorefineries from lignocellulosic biomass, integrating the coproduction of biofuels and/or value-added chemicals from the different biomass components has become a target to reach economic self-sustainability as well as get an efficient exploitation of the natural resources. For instance, second generation biofuels plants commonly coproduce power and biogas using the solid residues obtained during the cellulosic biofuel production and waste treatment processes (Cesaro and Belgiorno, 2015).

Cellulose nanomaterials (CNM) are nano-sized particles which can be obtained from any type of cellulosic feedstock such as hardwoods, softwoods, grasses, and algae, or derived from bacterial cellulose. Also, CNM can be extracted from agricultural wastes (e.g. bagasse, straw, husk) generated from industrial production of starch, sugar and juices (Cho et al., 2020). These types of materials have emerged as a promising material in many sectors due to their attractive properties such as non-toxic nature, biocompatibility, and biodegradability (Lou et al., 2020; Michelin et al., 2020). Cellulose nanofibers (CNF) are commonly isolated from cellulosic materials by mechanical fibrillation, which includes the use of equipment such as high-pressure homogenizer or microfluidizer, high-speed blender, grinder, ball milling, extruder, and ultrasonicator (Espinosa et al., 2019; Michelin et al., 2020). One of the major disadvantages of mechanical treatment is the high energy consumption associated to the process. Previous reported studies have shown a reduction on the energy requirements during mechanical fibrillation when an enzymatic and/or chemical stage was introduced to the process (Bauli et al., 2019). However, employing enzymes to obtain CNF has attracted much attention in the past years owing to their high

specificity and environmentally friendly condition compared to chemical pretreatment. Besides, the existing acid hydrolysis methods for CNM production results not compatible with the biorefinery process because the processing of the highly acidic hydrolysate obtained represents a major challenge.

Biofuels and/or value-added chemicals production strategies by fermentation from lignocellulosic biomass consist mainly of the usage of both hexose and pentose sugars extracted from the biomass carbohydrate components. Hydrolysis of lignocellulosic biomass breaks down the cellulose fraction into glucose and the hemicellulose fraction into pentoses (e.g. xylose, arabinose) and hexoses (e.g. glucose, galactose, mannose). Since these sugars can be fermented to biofuels or other value-added chemicals using various microorganisms, the integration of CNM production along with coproducts implies that the recovery of fermentable sugars during CNM extraction should be addressed. Despite of this, reported data on efficient integration of CNM production with other value-added chemicals are still scarce. Generally, endoglucanases are the hydrolytic cellulases mostly employed for CNF production to avoid excessive cellulose depolymerization, since they attack the amorphous cellulose chains to produce chain ends (Siqueira et al., 2019; Berto et al., 2021). Thus, enzymatic pretreatment results in low soluble sugars release which, if the integrated production of CNF and biofuels or value-added chemicals is intended, it is not desired. To overcome this, the introduction of a combined cellulase-cocktail containing endoglucanases along with exoglucanases/cellobiohydrolases and β-glucosidase/cellobiases followed by mechanical treatment is proposed, in which the enzymes mixture can degrade amorphous and crystalline regions without significantly compromising the cellulose fraction before the cellulose is nanofibrillated by mechanical shear. A suitable control of the enzyme loading, operational conditions, and cellulase-cocktails composition could allow a high process

control of the degradation level of the different solid components, especially the cellulose fraction. This would prevent an extensive cellulose hydrolysis which could negatively affect the CNF extraction yield, and also enable the possibility to recover a separate sugar stream that could be valorized.

Biobutanol, a downstream product of biomass-derived sugar processing, represents an important liquid biofuel. It has gained great interest as a fuel additive owing to its high energy content, good compatibility with engines, and low emissions (Cao et al., 2020). Moreover, it has recently attracted more attention because of its advantages over other bioalcohols (e.g. ethanol and methanol), such as high tolerance to water contamination, ability to blend in gasoline or diesel without phase separation, less corrosive to fuel system (Li et al., 2018). In addition to its role as an alternative to fossil fuels, butanol serves as an important platform chemical with applications such as a solvent, precursor for paints, and polymers formulation, among others (Birgen et al., 2019). It can be produced by fermentation from pentose and hexose sugars through the so-called ABE (acetone-butanol-ethanol) or IBE (isopropanol-butanol-ethanol) fermentation, in which butanol and coproducts (acetone, isopropanol and ethanol) are simultaneously produced. The most commonly wild type microorganisms employed for biobutanol fermentation include *Clostridium beijerinckii* strains (Veza et al., 2021). However, these strains may produce low butanol concentration and yields because of butanol inhibition and coproducts formation (Cebreiros et al., 2021a; Cho et al., 2020).

In this context, the aim of this study was to evaluate the feasibility of integrating the extraction of cellulose nanofibers (CNF) through enzyme-mediated pretreatment with the production of biobutanol by sugar fermentation from bleached eucalyptus Kraft pulp (BEKP). BEKP was selected as cellulosic feedstock in this work due to the high production and availability from the pulp and paper industry. For the CNF extraction, ball

milling was employed as mechanical treatment because of its ease of use, applicability to different types of materials, and relatively inexpensive equipment. Considering that CNF applications strongly depend on their properties, the effects of enzymatic pretreatment parameters on the main properties of the extracted CNF were investigated. Also, cellulose-derived and hemicellulose-derived sugars released during enzymatic pretreatment of BEKP using cellulase and xylanase enzymes was investigated. These fermentable sugars streams obtained as coproduct were further valorized by fermentation for biobutanol production using *Clostridium* strains. This study highlights the promising opportunity to produce value-added chemicals from the sugars generated during CNF extraction by enzyme-mediated pretreatment from cellulosic materials. To the best of the authors' knowledge, there are no previous studies on the implementation of enzymatic and microbial bioconversion of eucalyptus pulp to coproduce CNF and biobutanol.

## 2. Materials and Methods

### *2.1. Raw material, enzymes, and strains*

Bleached eucalyptus Kraft pulp (BEKP) was supplied by UPM (Fray Bentos, Uruguay). Major chemical components determined following TAPPI standard method T222 were cellulose (77.3 ± 0.6%) and xylan (17.6 ± 0.1%). The enzymatic cocktail used was prepared by employing equal amounts on mass basis of cellulase Cellic CTec3 (Novozymes, Davis Carolina) and xylanase Cellic HTec (Novozymes, Davis Carolina) according to Cebreiros et al. (2021b). The total protein content and filter paper activity of the enzymatic cocktail was 166 mg/mL and 183 FPU/mL, respectively. *Clostridium beijerinckii* DSM 6422 and *Clostridium beijerinckii* DSM 6423 were purchased from DSMZ (Leibniz, Germany) and manipulated as previously described (Cebreiros et al., 2021a).

### *2.2. Enzymatic pretreatment of BEKP*

Suspensions containing 4%, 10% and 16% (w/w) of BEKP were enzyme-treated at 50°C and pH 4.8 (acetate buffer 50 mM) with an enzyme loading of 5 FPU/$g_{solid}$ and orbital agitation (150 rpm) during 4 h and 8 h (see Table 1). After enzymatic pretreatment, the enzyme was deactivated by heating at 100°C for 10 min. The liquid (enzymatic hydrolysate) and solid (cellulose fibers) fractions were then separated by centrifugation (5,000 rpm for 15 min). The cellulose fibers were re-suspended in distilled water and washed three times by centrifugation before storage at 4°C for further processing. Solid yield (SY, wt%) was calculated based on the amount of oven-dried mass of substrate (BEKP) and cellulose fibers recovered after enzymatic pretreatment.

**Table 1.** Enzymatic pretreatment conditions evaluated using an enzyme loading of 5 FPU/$g_{solid}$.

| **Sample** | *Enzymatic hydrolysis conditions* | |
|---|---|---|
| | **Solid concentration (wt%)** | **Hydrolysis time (h)** |
| HE4-4h | 4.0 | 4 |
| HE4-8h | 4.0 | 8 |
| HE10-4h | 10.0 | 4 |
| HE10-8h | 10.0 | 8 |
| HE16-4h | 16.0 | 4 |
| HE16-8h | 16.0 | 8 |

### *2.3. Mechanical treatment for CNF extraction*

Ball milling was performed at room temperature in a laboratory ball mill (MM 400, Retsch) for CNF extraction. For this, 10 mL of 1% (w/w) enzymatically pretreated cellulose fibers suspension was loaded onto a 25 mL-zirconia grinding jar containing

zirconia balls of 0.5 mm and 3 mm in diameter with a ball to solid ratio (BSR) of 80 $g_{balls}/g_{dry\ solid}$. Balls of 0.5 mm and 3 mm in diameter were used at a mass ratio of 7:3. Ball milling was performed at 20 Hz for 1.5 h. After the milling process, balls separation was performed by mesh filtration. Since the slurry was gel-like and sticky, distilled water was added to the slurry until a consistency of 0.2% (w/w) to facilitate balls separation.

### *2.4. Biobutanol fermentation*

Fermentations assays were performed in 100-mL bottles containing 40 mL of enzymatic hydrolysate under anaerobic conditions. The fermentation media were supplemented with yeast extract (1 g/L) and P2 stock solutions (1% v/v) according to previous work (Cebreiros et al., 2021a). The bottles were inoculated with 10% (v/v) active cells from the fermentation inoculum, which was prepared as previously described (Cebreiros et al., 2021a). The initial pH of the media was adjusted to 6.0 ± 0.1. Control fermentations were also performed using semi-synthetic media containing glucose and xylose at the same concentrations to those found in the enzymatic hydrolysates. Fermentation assays were carried out at 35°C with orbital agitation (150 rpm) for 72 h in duplicate. Dry cell mass (X) was determined by optical density (OD) at 600 nm considering that one unit of $OD_{600\ nm}$ corresponded to 0.33 ± 0.02 g/L of X and 0.38 ± 0.03 g/L of X for *C. beijerinckii* DSM 6422 and *C. beijerinckii* DSM 6423, respectively.

### *2.5. Analysis of enzymatic hydrolysates and fermentation samples*

Chemical analysis of enzymatic hydrolysates from enzymatic pretreatment was performed following NREL protocol (NREL/TP-510–42623) for liquid fractions. Monomeric sugars were determined by HPLC (Shimadzu, Kyoto, Japan) equipped with a refractive index detector (RID) and an Aminex HPX-87H column (Bio-Rad Laboratories Ltd., USA), which operated at 45°C and 0.6 mL/min using 5 mM $H_2SO_4$ as

mobile phase. Butanol, acetone, isopropanol, ethanol, acetic acid, and butyric acid were quantified by GC (Shimadzu GC-2010) using a flame ionization detector and a fused silica column (RTX®-Wax, 0.5 μm film thickness, 30 m long, and 0.32 mm ID, Restek).

### *2.6. Characterization of cellulose fibers from enzymatic pretreatment*

Water retention value (WRV) was used to determine the fiber fibrillation extent and swelling in cellulose fibers after enzymatic pretreatment using the TAPPI UM256 as described elsewhere (Cebreiros et al., 2021b). Adsorption experiments using Direct Blue dye (DB) were performed as previously described (Cebreiros et al., 2021b) to estimate the total cellulose surface area in solid fractions. The degree of polymerization (DP) of BEKP and cellulose fibers after enzymatic pretreatment was determined according to TAPPI standard method T230 by viscosity of fiber solution in 0.5 M cupriethylenediamine (CED) solution as previously described (Cebreiros et al., 2021b). Conductometric titration was performed to determine the BEKP and cellulose fibers acidic groups content according to Katz and Beatson (1984). Briefly, 50 mL of 0.001 M NaCl solution was added to 0.25 g (oven-dry basis) of sample and the pH was adjusted to 3.0 ± 0.1 using 0.1 M HCl. Then, titration of the suspension was performed using 0.05 M NaOH, and the conductivity values were recorded. X-ray diffraction (XRD) analysis was performed in a Philips PW1700 diffractometer with CuKα radiation operated at 30 kV and 40 mA, with a scanning rate of 0.02°/s and 2θ range of 0° to 60°, to determine the cellulose fibers crystallinity index (CrI) according to Segal et al. (1959).

### *2.7. Characterization of CNF suspensions*

Zeta Potencial (ZP) and Dynamic Light Scattering (DLS) analysis of CNF colloids were performed using a Malvern Zetasizer Nano-ZS (Malvern Instruments Inc.), previously diluted to 0.01 wt%. The light transmittance of CNF suspensions (0.1 wt%)

was measured in the range of 300-800 nm using Genesys 10S UV-Vis spectrophotometer. CrI of CNF samples was determined by XRD analysis, as described above. TEM analysis was performed using a Jeol JEM 1010 transmission electron microscope operated at 100 kV. Briefly, 10 µL of 0.01 wt% CNF suspension was deposited onto carbon-coated copper grid with formvar/carbon film and, after ambient drying, 10 µL of 2% uranyl acetate solution was deposited on the grid to negatively stain the sample. ImageJ software was used to estimate CNF widths from over 100 individual CNF. Sedimentation experiments of CNF suspensions were performed to calculate the relative aspect ratios of the CNF samples from gel point concentrations. Briefly, a series of diluted CNF suspensions of 0.15, 0.1, 0.05, 0.025 and 0.01% (1.5, 1.0, 0.5, 0.25 and 0.1 $kg/m^3$) were prepared and allowed to settle for 48 h. Photographs were taken before and after sedimentation to determine the sedimentation ratio ($h_s/h_o$) as the ratio of sediment height ($h_s$) to initial suspension height ($h_o$) using ImageJ software. An estimated gel point concentration was calculated by plotting fiber concentration against sedimentation ratio and determining the derivative of the trendline equation, following the methodology reported by other authors (Raj et al., 2016; Varanasi et al., 2013). The Crowding Number theory described by Martinez et al. (2001) was used to calculate the aspect ratio, which determines the gel point and aspect ratio of cellulose pulp fibers assuming a density of fibers around 1500 $kg/m^3$ (Varanasi et al., 2013).

## 3. Results and discussion

### *3.1. Enzymatic hydrolysis and sugar yields*

Fig. 1 shows the results obtained after enzymatic pretreatment for the conditions evaluated (Table 1). It was clearly observed that the cellulose and xylan conversion yields decrease with increasing solid loadings, which was also reported in several previous

studies (Cebreiros et al., 2021b; da Silva et al., 2020; Pereira and Arantes, 2020). However, this may be alleviated with an increased reaction time. For instance, higher cellulose and xylan conversions of the cellulose-rich BEKP were reached at 4% solid loading when hydrolysis was performed for 4 h (43% and 68%, respectively) and 8 h (53% and 80%, respectively). Even though lower cellulose and xylose conversions were achieved at 10% solid loadings after 4 h of hydrolysis (30% and 55%, respectively), these results were further increased when hydrolysis was performed for 8 h (56% and 82%, respectively). Thus, comparable results were achieved both at 4% and 10% solid loadings when performing enzymatic hydrolysis for 8 h. On the other hand, enzymatic hydrolysis at higher solid loading (16% w/w) for 8 h resulted in cellulose and xylan conversions of 35% and 59%, respectively, which represents a decrease of 26% to 37% on conversion rates.

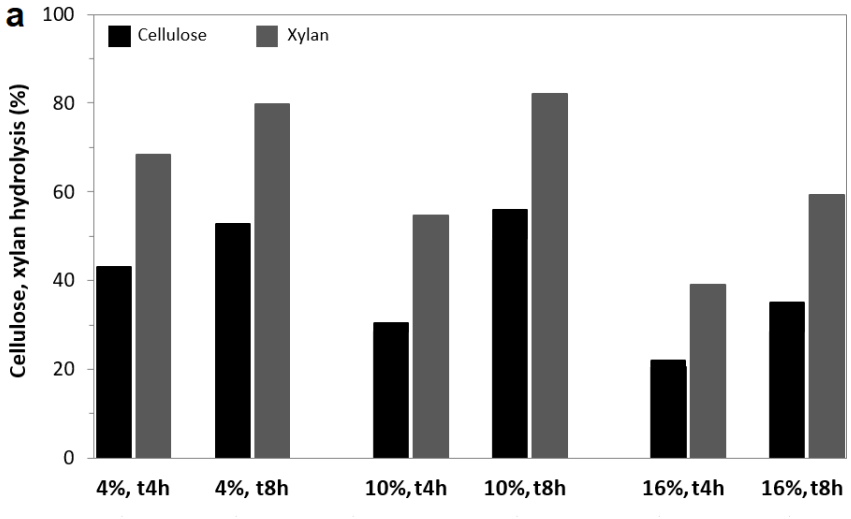


223

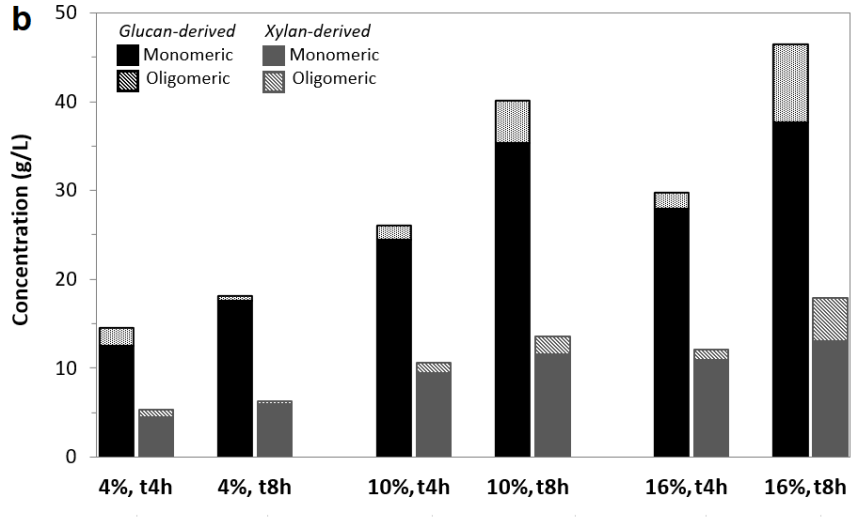


224

225 **Fig 1.** Cellulose (as glucan) and xylan hydrolysis efficiency (a), and glucan-derived and
226 xylan-derived sugars concentrations in monomeric and oligomeric forms (b) obtained
227 after enzymatic pretreatment of BEKP under the different conditions evaluated.

228 Despite cellulose and xylan conversion decrease with higher solid loadings, higher
229 glucan-derived and xylan-derived sugars concentrations were achieved under these
230 conditions. For instance, glucose (15-20 g/L) and xylose concentrations (5 g/L) reached
231 at 4% solid loading resulted two-fold lower than glucose (30-45 g/L) and xylose (10-
232 15 g/L) concentrations achieved at 16% solid loading. However, by increasing the solid
233 loading from 10% to 16% only an increase of 20% was observed on the glucose and

xylose concentrations, while an increase of 120% was observed by increasing the solid loading from 4% to 10% (Fig. 1). This may be explained by the significant reduction on the carbohydrate conversion rates by further increasing the solid concentration of the slurry.

High monosaccharides (e.g. glucose, xylose) concentrations are desirable for a biochemical platform process converting cellulosic feedstocks into high value-added chemicals. Because of this, enzymatic hydrolysates samples containing a total sugar (glucose and xylose) concentration higher than 20 g/L were subsequently utilized to produce biobutanol by *Clostridium* fermentation. It was also observed that the amount of sugars in oligomeric form which were released during enzymatic pretreatment was relatively low (<30%) in all cases (Fig. 1). This could be due to the efficient performance of the enzyme preparations used in this study that were specifically developed for biomass deconstruction into monomeric sugars.

### *3.2. Characterization of cellulose fibers after enzymatic pretreatment*

The solid residues (cellulose fibers) recovered after enzymatic pretreatment were characterized to evaluate changes and/or modifications occurring during pretreatment to the cellulose fibers in the original BEKP (Table 2). The cellulosic substrates were characterized for cellulose accessibility using WRV and DB adsorption assays. At fiber level, the overall porosity was assessed by the WRV, which provides an estimation of the amount of water that can be retained by the inner pores of a cellulosic substrate and, thus, a relative indication of the fiber swelling capability. As fibers swell, they become more easily defibrillated, and a greater surface area is being exposed (Chen et al., 2013). The accessible surface area of cellulose was estimated by DB adsorption assays. Both the WRV and DB adsorption values of the different cellulose fibers recovered increased,

compared to the control BEKP (2.7 and 87.0, respectively), indicating an enhanced overall cellulose accessibility after the enzymatic pretreatment stage. During enzymatic hydrolysis, microfibers highly ordered regions are supposed to be disrupted and delaminated, causing a porosity increase as enzyme action opened up their structure (Meng et al., 2016). Samples HE4-4h (4.1), HE4-8h (4.3) and HE10-8h (4.0) had the highest WRV, which may indicate a greater exposure of cellulose chains that improved the water retention capability. Also, the highest DB adsorption values were reached for the samples HE4-4h (130) and HE4-8h (123), which remained almost unchanged, and sample HE10-8h (122). These results correspond quite well with the higher sugar conversion rates achieved under these conditions (4% and 10% solid loadings, 8 h hydrolysis, Fig. 1). The enhanced DB adsorption and water retention could be due to a reduction in the fiber aggregation degree caused by the enzymes, which increases the external surface area and, thus, causes a greater exposure of cellulose chains. Also, since amorphous regions occur between microfibers, cellulase pretreatment may lead to a swelling of the cellulose fibers which may cause an improved accessibility towards solvents and/or reagents, thus improving overall cellulose accessibility (Engström et al., 2006; Cebreiros et al., 2021b). It was also reported by other authors that enzyme-mediated pretreatment increases external surface area through external fibrillation, which increases fiber water retention (Gu et al., 2018). According to these results, a higher fiber fragmentation was expected for samples HE4-4h, HE4-8h, and HE10-8h, which could be related to the greater xylan hydrolysis under these conditions (Fig. 1), since the lower xylan content on the fibers surface could have facilitated the accessibility of the enzyme to cellulose (Cebreiros et al., 2021b).

**Table 2.** Solid, glucose, and xylose yields, and characterization of cellulose fibers after enzymatic pretreatment.

| Sample | SY (%) | Glucose yield (g/100 $g_{BEKP}$) | Xylose yield (g/100 $g_{BEKP}$) | WRV | DB adsorption ($g/g_{dry\ solid}$) | AG (mmol/ $kg_{dry\ solid}$) | DP | CrI |
|---|---|---|---|---|---|---|---|---|
| BEKP | na | na | na | 2.7 | 87.0 | 44.2 | 1196 | 75.7 |
| HE4-4h | na | 31.9 | 11.6 | 4.1 | 130 | 65.4 | 332 | nd |
| HE4-8h | 52.2 | 43.9 | 15.3 | 4.3 | 123 | 77.3 | 288 | 79.2 |
| HE10-4h | 42.8 | 24.5 | 9.7 | 3.5 | 108 | 58.8 | 345 | nd |
| HE10-8h | 65.0 | 42.3 | 14.0 | 4.0 | 122 | 75.2 | 258 | 78.2 |
| HE16-4h | 39.2 | 17.7 | 7.1 | 3.5 | 88.6 | 48.7 | 524 | nd |
| HE16-8h | 74.9 | 24.5 | 8.6 | 3.6 | 98.2 | 66.2 | 458 | 77.4 |

SY: solid yield; WRV: water retention value; DB: direct blue; AG: acidic groups; DP: degree of polymerization; CrI: crystallinity index; na: not applicable; nd: not determined.

Besides, even though enzyme-mediated pretreatment contributes to the fibers fibrillation, it was previously reported that the enhanced fiber swelling can be related to an increased acidic groups content in the pulp (Chen et al., 2013). These acidic groups, which are associated with the carboxyl groups of the cellulosic fibers, causes electrostatic repulsion between the carboxylate anions and, thus, fiber swelling (Moser et al., 2015). As shown in Table 2, the acidic groups content and WRV values present the same changing trend, which was also reported by other authors (Chen et al., 2021; Chen et al., 2013). One possible explanation to the increased WRV value could be the introduction of acidic groups by enzymatic pretreatment, since the swelling of the fibers can be enhanced with increasing fiber charge.

DP is also an important parameter which evaluates the cellulose chains length, as it is defined as the number of repetition times of the monomeric unit that constitutes the polymer chain (Meng et al., 2016). Table 2 presents the variations on cellulose DP for the

different cellulosic residues. Enzymatic hydrolysis resulted in a significant reduction (>50%) in DP for all the pretreatment conditions evaluated. This drastic decrease in DP was expected since it was already reported that enzymatic hydrolysis using cellulases causes shortening in the cellulose chains length and, thus, a decrease on the cellulose molecular weight distribution. For instance, Ramos et al. (1993) reported DP values of 268-220 after enzymatic hydrolysis of peroxide pretreated eucalyptus, achieving a 40% DP reduction after 10 h. Moreover, it was possible to determine the CrI of cellulose fibers from XRD analysis. During enzymatic hydrolysis, amorphous or disordered segments in cellulose is generally believed to be hydrolyzed at a faster rate compared to crystalline or ordered segments in cellulose. Because of this, it was expected an increase on CrI after enzymatic pretreatment. A slight increase (2-5%) was observed compared to the control BEKP (CrI 75.7±0.5%) after 8 h of enzymatic hydrolysis (Table 2). Considering that cellulose hydrolysis extent was apparent for all the conditions evaluated according to conversion rates (Fig. 1), this result may suggest that amorphous and crystalline regions in the fibers were partially hydrolyzed at similar rates, without causing significant changes in the CrI.

### *3.3. Extraction and characterization of CNF suspensions*

Table 3 presents the main characterization results for the CNF suspensions obtained after ball milling from each experimental condition employed during enzymatic hydrolysis. One of the main challenges in the characterization of fibrillated materials is that the fibrils size and aspect ratio are hard to determine accurately using traditional microscopy, since the fibrils form a complex and entangled network. Because of this, the DLS method was used for a more integral evaluation of the size distribution of CNF suspensions, while a relatively simple gel point determination technique was proposed to estimate the fibrils aspect ratio. Even though several studies used this method to

determine the approximate relative aspect ratios of micro/nanofibrillated cellulose fibers (Varanasi et al., 2013; Gourlay et al., 2018; Sanchez-Salvador et al., 2021), the calculated aspect ratio should not be considered as the true average aspect ratio of a sample, but as relative values to compare between samples that were produced employing different pretreatment conditions. Also, DLS method should be used in combination with other methods when comparing different samples.

**Table 3.** Characterization of CNF suspensions extracted from enzyme-treated BEKP by mall milling treatment.

| CNF sample | Average hydrodynamic size (nm) | PDI[a] | Zeta Potential (mV) | Aspect ratio | Transmittance at 800 nm (%) |
|---|---|---|---|---|---|
| BM(HE4-4h) | 1116 ± 87 | 0.76 ± 0.11 | -10.5 ± 1.6 | 222 | 39.7 |
| BM(HE4-8h) | 535 ± 19 | 0.35 ± 0.05 | -15.5 ± 0.6 | 220 | 50.0 |
| BM(HE10-4h) | 1321 ± 301 | 0.78 ± 0.23 | -14.8 ± 0.3 | 189 | 39.2 |
| BM(HE10-8h) | 942 ± 162 | 0.43 ± 0.13 | -12.3 ± 0.4 | 227 | 49.1 |
| BM(HE16-8h) | 2435 ± 209 | 0.92 ± 0.09 | -9.5 ± 0.2 | 144 | 33.8 |

PDI: polydispersity index
[a]Values < 0.7 are considered homogeneous

The determination of the average hydrodynamic size and the PDI gives an indication of the presence of agglomerates and/or large particles and the degree of size homogeneity in the sample, respectively. According to DLS analysis of the ball milled samples, average hydrodynamic sizes resulted within the range of 500 nm to 2.4 µm for all the conditions evaluated. Considering that average hydrodynamic sizes higher than 25 µm (data not shown) were determined for the enzyme-treated materials before mechanical treatment, DLS results demonstrated that ball milling treatment contributes to fiber size reduction and CNF extraction. This considerable fiber fragmentation results from the high shear

forces produced from the balls collisions and the friction between the balls and the container wall. Differences on the average hydrodynamic sizes of the CNF samples indicates that both solid loading (4%, 10% and 16%) and reaction time (4 h and 8 h) conditions during enzymatic hydrolysis influenced subsequent fiber fragmentation and/or fibrillation by ball milling through fiber structure alterations. It can be observed that the lowest fiber fragmentation and highest PDI value was obtained for sample BM(HE16-8h). This indicates the presence of larger particles which could be due to incomplete fiber fragmentation, and, thus, low cellulose nanofibrillation degree. On the other hand, it can be observed that fiber surface changes that occurred during enzymatic hydrolysis performed at 4% and 10% solid loadings, which corresponds to samples BM(HE4-4h), BM(HE4-8h), BM(HE10-4h), and BM(HE10-8h), enhanced fiber size reduction by subsequent ball milling. Extending the enzymatic hydrolysis time from 4 h to 8 h provided higher fiber fragmentation (average sizes in the nanoscale range -500 to 900 nm-) which favored the extraction of CNF, since decreases of 30% to 50% on the average size was observed. The PDI also decreased (0.35-0.43), indicating a greater CNF size homogeneity.

The determination of the CNF aspect ratio gives an indication of the separation and breakage extent of cellulosic fibers by estimating the ratio of the longest side to the shortest side. Even though the breakage of fibers is more apparent during ball milling treatment, enzymes act mostly in the amorphous regions of cellulose during enzymatic pretreatment, which cuts the cellulose chains and reduces their length. Because of this, even though the applied ball milling conditions were the same for all the samples, the aspect ratio values resulted different (Table 3). The aspect ratio values presented a more pronounced increase for samples BM(HE4-4h), BM(HE4-8h), and BM(HE10-8h), which reached values higher than 220, probably because of a decrease in the microfiber diameter

due to peeling. Also, this could be associated to a better fibrillation of these cellulose fibers through ball milling treatment, which has been previously explained by the easier fragmentation due to fiber alterations during enzymatic hydrolysis. No significant difference was observed between samples BM(HE4-4h) and BM(HE4-8h) in terms of aspect ratio value, even though DLS results showed an increased fiber fragmentation for sample BM(HE4-8h) given the lower average hydrodynamic size (535 nm). This could be due to the fact that during ball milling, not only are microfibers separated but also shortened, which means that the length and the diameter of the extracted CNF decreased in a similar proportion resulting in a similar aspect ratio. On the other hand, it can be observed by comparing samples BM(HE10-4h) and BM(HE10-8h) that the aspect ratio increased with the enzymatic hydrolysis time probably because of a predominant fibrillation effect, reaching a value of 227. Thus, these results may indicate that cellulosic samples HE4-4h, HE4-8h and HE10-8h resulted more processable during ball milling treatment, since the aspect ratio values of samples BM(HE4-4h), BM(HE4-8h) and BM(HE10-8h) resulted higher compared to samples BM(HE10-4h) and BM(HE16-8h). The lower aspect ratio values of samples BM(HE10-4h) and BM(HE16-8h) could be attributed to the higher hemicellulose content in these samples, since it was reported by other authors that hemicellulose could apply a strong holding of fiber bundles, preventing them from becoming smaller after ball milling (Sanchez-Salvador et al., 2021; Cebreiros et al., 2021b). Thus, it may be possible that a greater removal of hemicellulose during enzymatic hydrolysis facilitated the peeling of the cellulosic fibers during ball milling.

ZP determinations were performed based on the tracking of the moving rate of positively or negatively charged particles across an electric field. The ZP of the CNF suspensions varied from -15 mV to -10 mV (Table 3), which indicates that they form an unstable colloidal suspension. Usually, ZP values below -15 mV represents the beginning

of agglomeration, and values above -30 mV are considered desirable for good colloidal stability (Zhou et al., 2012). However, the ZP values registered were expected, since unlike other methods such as acid hydrolysis, enzymatic pretreatment does not incorporate negatively charged groups on the cellulose surface. The produced CNF has only a weak charge of around -15 mV, which came from its inherent hydroxyl groups. The absence of strong charges on the cellulose surface does not prevent aggregation of the CNF, which may induce agglomeration of the CNM, resulting in a wide size dispersion (Table 3). These findings result in agreement with previous studies using enzymatic pretreatment for the extraction of CNM (nanocrystals or nanofibers) (Squinca et al., 2020; Zhou et al., 2012). However, it should be mentioned that materials with lower negative ZP values were reported more acceptable for biomedical and related applications (Squinca et al., 2020).

Spectroscopic methods have been employed as an indirect method to evaluate the fibrillation extent by measuring the transmittance or turbidity of the suspension (Foster et al., 2018). The increase of transmittance at a specific wavelength indicates the presence of more homogeneous and/or smaller materials in the nanoscale range. Moreover, it was previously reported a good correlation between transmittance and CNF gravimetric yield determined by centrifugation method. Thus, it is possible to correlate the fibrillation extent directly to the transmittance (Moser et al., 2015). However, it is difficult to use this rapid measurement alone to determine fiber disintegration since nanomaterials are released simultaneously with detectable particles when mechanical disintegration is performed (Moser et al., 2015). Transmittance values at 800 nm are presented in Table 3 for CNF samples obtained. These values ranged from 34% to 50%, achieving the highest value for samples BM(HE4-8h) and BM(HE10-8h). Transmittance results correspond quite well with the DLS analysis, which indicated that a higher fiber fragmentation was

achieved for these samples considering the lower average hydrodynamic sizes (500-1000 nm) and PDI values (0.3-0.4) compared to the other samples. Also, results showed that extending the enzymatic hydrolysis time from 4 h to 8 h allowed to achieve a better fibrillation extent during ball milling process.

The crystallinity of CNF samples BM(HE4-8h) and BM(HE10-8h) was not significantly influenced by ball milling treatment (CrI 81-83%) when comparing to the cellulosic samples before ball milling (76-79%). This shows that the ball milling did not cause significant impact on the crystalline structure of CNF. Moreover, the morphology of the CNF extracted from enzyme-treated BEKP observed in TEM micrographs showed entangled networks with fibril diameters in the nanoscale range (Fig. 2). The CNF sample extracted by ball milling after 8 h of enzymatic hydrolysis (sample BM(HE10-8h)) presented an average width of 8.0 ± 0.2 nm (Fig. 2c). TEM analysis demonstrates that the pretreatment conditions used in this study resulted effective to provide a significant diameter reduction of the untreated BEKP, which was about 25.1 μm (Cebreiros et al., 2021b).

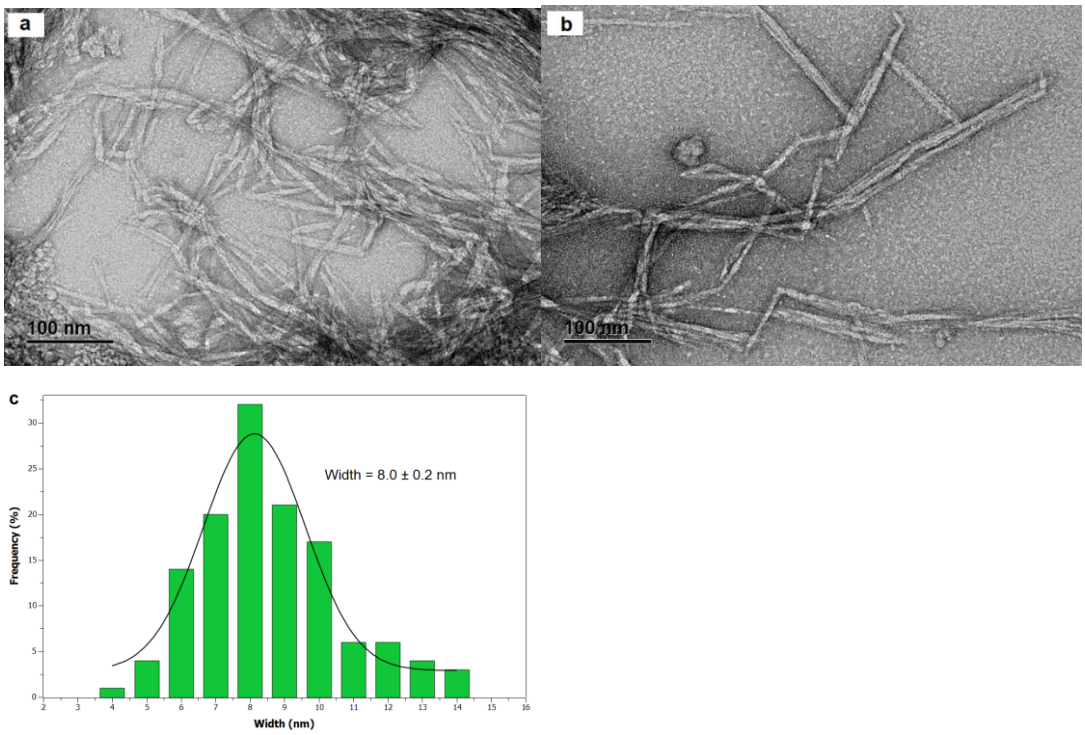


**Fig 2.** TEM images (a,b), and width distribution (c) of CNF extracted from enzyme-treated BEKP (sample HE10-8h). Average width and standard deviation are presented in the figure.

### *3.4. Biobutanol fermentation of enzymatic hydrolysates*

Glucose and xylose consumption, biomass growth, and butanol and solvents production profiles during biobutanol fermentation in all experiments are shown in Fig. 3. For ABE fermentation, it can be observed complete consumption of both glucose and xylose within 24-48 h of incubation. It should be noted that lower initial sugars concentrations (20-35 g/L) required less than 24 h to be completely consumed, while higher sugars concentrations (50 g/L) required up to 48 h. Higher amounts of butanol and solvents (acetone and ethanol) were produced when the concentration of sugars in the medium was higher. The highest butanol concentration of 8.9 g/L (14 g/L total solvents) was achieved after 48 h in the enzymatic hydrolysates (HE10-2 and HE16-2) containing initially 41-43 g/L of sugars. Acetone (5.3 g/L) and ethanol (0.35 g/L) were also

coproduced during fermentation but in lower concentrations. Regarding biomass growth, biomass concentrations of 1.4-2.4 g/L were achieved after 24 h for all the experiments, with the highest growth (2.3 g/L) observed in samples with high initial sugar concentration. Table 4 presents the fermentation parameters determined after 24 h and 48 h when corresponded, for each experiment. One of the main advantages of *Clostridium* strains are their ability to ferment different types of substrates derived from lignocellulosic materials including hexoses and pentoses such as glucose, xylose, cellobiose, etc. (Cebreiros et al., 2021a). In this study, high consumptions rate of both glucose (up to 100%) and xylose (up to 96%) were achieved for all the conditions evaluated using enzymatic hydrolysates. Moreover, these consumptions rates resulted higher compared to those achieved in the experiments using semi-synthetic media (87-100% for glucose, 31-78% for xylose). It should be noted that a higher concentration of initial acetic acid was observed in the enzymatic hydrolysate samples (up to 4 g/L) than in the semi-synthetic media (up to 2.5 g/L), which may be possibly due to the acetate buffer used during enzymatic pretreatment. According to previous studies (Cebreiros et al., 2021a), the higher acetate concentration in the enzymatic hydrolysates could have enhanced butanol fermentation performance and, thus, sugars consumption, improving overall butanol yields (0.20-0.21 g/g).

**Table 4.** Butanol fermentations of hydrolysates obtained from enzymatic pretreatment and semi-synthetic media by *C. beijerinckii* DSM 6422.

| Parameter | Enzymatic hydrolysate | | | | Semi-synthetic medium | | |
|---|---|---|---|---|---|---|---|
| | **HE4-8h** | **HE10-4h** | **HE10-8h** | **HE16-8h** | **S1** | **S2** | **S3** |
| $t_F$ (h) | 24 | 24 | 48 | 48 | 48 | 24 | 24 |
| $G_i$ (g/L) | 16.7 | 19.7 | 30.4 | 31.3 | 36.8 | 26.1 | 15.2 |
| $X_i$ (g/L) | 5.5 | 8.4 | 11.3 | 11.2 | 13.4 | 9.6 | 5.3 |
| $C_G$ (%) | 100 | 100 | 100 | 100 | 92 | 87 | 100 |
| $C_X$ (%) | 93 | 93 | 96 | 90 | 31 | 46 | 78 |
| B (g/L) | 4.6 | 6.1 | 8.9 | 8.9 | 7.4 | 6.7 | 3.7 |
| AE (g/L) | 3.0 | 3.6 | 5.6 | 5.3 | 5.2 | 2.6 | 2.5 |
| ABE (g/L) | 7.6 | 9.7 | 14.5 | 14.2 | 12.6 | 9.3 | 6.2 |
| HAc (g/L) | 1.6 | 1.1 | 0.7 | 0.7 | 0.7 | 0.5 | 0.8 |
| Hbu (g/L) | 1.2 | 1.0 | 0.9 | 0.5 | 0.3 | 0.4 | 1.0 |
| ΔX (g/L) | 1.6 | 1.9 | 2.2 | 2.3 | 2.3 | 1.8 | 1.3 |
| $Y_{B/S}$ (g/g) | 0.20 | 0.21 | 0.21 | 0.21 | 0.19 | 0.19 | 0.18 |
| $Y_{ABE/S}$ (g/g) | 0.32 | 0.33 | 0.34 | 0.33 | 0.32 | 0.28 | 0.29 |
| $Q_B$ (g/Lh) | 0.19 | 0.25 | 0.18 | 0.18 | 0.15 | 0.22 | 0.16 |
| $Q_{ABE}$ (g/Lh) | 0.32 | 0.40 | 0.30 | 0.29 | 0.26 | 0.32 | 0.26 |
| Butanol:ABE[a] | 0.55 | 0.56 | 0.55 | 0.56 | 0.53 | 0.67 | 0.54 |

See Table 1 for more information on the conditions for obtaining the hydrolysates.
S1, S2, S3: semi-synthetic medium 1, 2 and 3, respectively; $t_F$: fermentation time; $G_i$: initial glucose concentration; $X_i$: initial xylose concentration; $C_G$: glucose consumption; $C_X$: xylose consumption; B: butanol; AE: acetone and ethanol; HAc: acetic acid; HBu: butyric acid; ΔX: overall biomass growth; $Y_{B/G}$: overall sugars to butanol conversion yield; $Y_{ABE/G}$: overall sugars to ABE conversion yield; $Q_B$: overall butanol productivity; $Q_{ABE}$: overall ABE productivity
[a]Produced butanol to ABE molar ratio

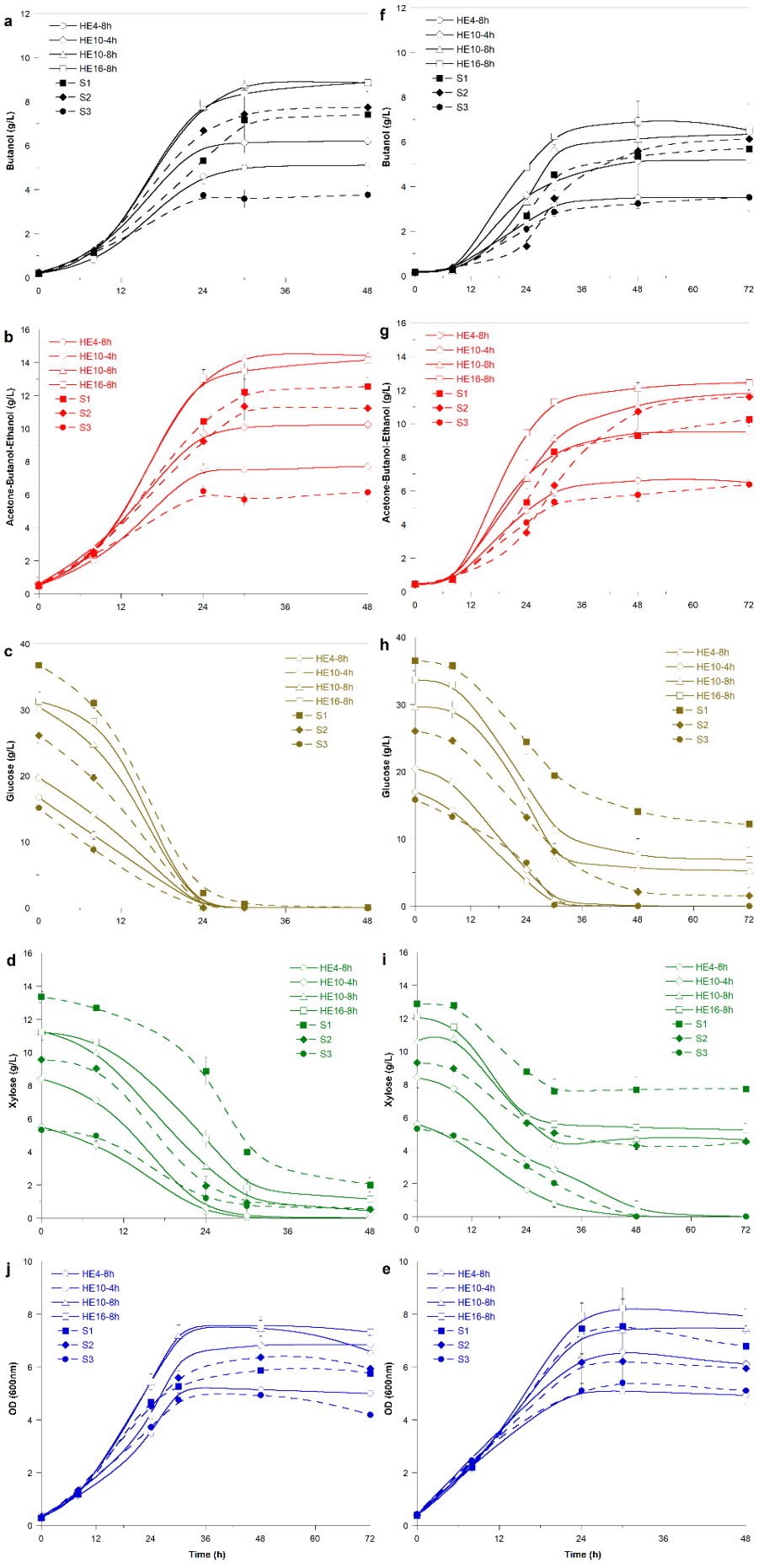
a
Butanol (g/L)
HE4-8h
HE10-4h
HE10-8h
HE16-8h
S1
S2
S3
f
Butanol (g/L)
b
Acetone-Butanol-Ethanol (g/L)
g
Acetone-Butanol-Ethanol (g/L)
c
Glucose (g/L)
h
Glucose (g/L)
d
Xylose (g/L)
i
Xylose (g/L)
j
OD (600nm)
e
OD (600nm)
Time (h)
Time (h)

**Fig 3.** Butanol (a, f), total ABE (b, g), glucose (c, h), xylose (d, i), and OD at 600 nm (e, j) profiles for ABE (a-e) and IBE (f-j) fermentation of enzymatic hydrolysates (HE4-8h, HE10-4h, HE10-8h, HE16-8h) and semi-synthetic media (S1, S2 and S3).

For IBE fermentation, the same trend was observed, the highest butanol concentration reached corresponded to the highest initial sugar concentration. The highest butanol concentration of 6.9 g/L (12 g/L total solvents) was achieved in this case after 48 h in the enzymatic hydrolysate (HE16-2) containing initially 46 g/L of sugars. Isopropanol (up to 5.5 g/L) was produced in this case instead of acetone, along with low concentrations of ethanol (up to 0.2 g/L). Regarding biomass growth, biomass concentrations of 1.4-3.0 g/L were achieved after 24 h for all the experiments, with the highest growth (2.9 g/L) observed in samples with high initial sugar concentration. Table 5 presents the overall parameters determined after 48 h for each experiment. In this case, high consumptions were not achieved in all the experiments. Only in experiments with relatively low initial sugar concentration (20-28 g/L) was achieved high consumption rates of glucose (92-100%) and xylose (81-100%). When initial sugar concentration was further increased (35-50 g/L), residual amounts of both glucose and xylose sugars remained unconverted (up to 27% for glucose and 56% for xylose). It should be noted that the amount of unconverted sugars resulted lower in the enzymatic hydrolysate samples rather than in the semi-synthetic media, probably due to the enhanced butanol fermentation performance at higher initial acetate concentration (Cebreiros et al., 2021a). Incomplete sugar conversion to butanol and coproducts in IBE fermentation was previously reported (Cebreiros et al., 2021a; Cebreiros et al., 2019) and others (dos Santos Vieira et al., 2021) IBE fermentation studies. Even though incomplete sugar consumption was not achieved at higher sugars concentration, higher butanol yields (0.20-0.21 g/g) were effectively achieved in this case.

**Table 5.** Butanol fermentations of hydrolysates obtained from enzymatic pretreatment and semi-synthetic media by *C. beijerinckii* DSM 6423.

| Parameter | Enzymatic hydrolysate | | | | Semi-synthetic medium | | |
|---|---|---|---|---|---|---|---|
| | **HE4-8h** | **HE10-4h** | **HE10-8h** | **HE16-8h** | **S1** | **S2** | **S3** |
| $t_F$ (h) | 48 | 48 | 48 | 48 | 48 | 48 | 48 |
| $G_i$ (g/L) | 17.0 | 20.4 | 29.7 | 33.7 | 36.5 | 26.0 | 15.8 |
| $X_i$ (g/L) | 5.6 | 8.4 | 10.6 | 12.1 | 12.9 | 9.3 | 5.3 |
| $C_G$ (%) | 100 | 100 | 81 | 77 | 73 | 92 | 100 |
| $C_X$ (%) | 81 | 94 | 56 | 55 | 44 | 54 | 100 |
| B (g/L) | 3.6 | 5.1 | 6.1 | 6.9 | 5.4 | 5.6 | 3.2 |
| IE (g/L) | 3.0 | 4.4 | 4.6 | 4.9 | 3.9 | 5.1 | 3.6 |
| IBE (g/L) | 6.6 | 9.5 | 10.7 | 11.8 | 9.3 | 10.7 | 5.8 |
| HAc (g/L) | 1.7 | 0.9 | 1.1 | 1.1 | 1.4 | 1.2 | 0.9 |
| Hbu (g/L) | 1.2 | 1.0 | 0.7 | 0.5 | 0.6 | 1.0 | 1.1 |
| $\Delta X$ (g/L) | 1.0 | 2.2 | 2.7 | 2.9 | 2.3 | 1.9 | 1.3 |
| $Y_{B/S}$ (g/g) | 0.15 | 0.18 | 0.20 | 0.21 | 0.16 | 0.19 | 0.15 |
| $Y_{IBE/S}$ (g/g) | 0.27 | 0.32 | 0.35 | 0.36 | 0.28 | 0.35 | 0.25 |
| $Q_B$ (g/Lh) | 0.07 | 0.11 | 0.13 | 0.14 | 0.11 | 0.12 | 0.07 |
| $Q_{IBE}$ (g/Lh) | 0.14 | 0.20 | 0.23 | 0.25 | 0.19 | 0.22 | 0.12 |
| Butanol:IBE[a] | 0.48 | 0.49 | 0.50 | 0.51 | 0.52 | 0.47 | 0.50 |

See Table 1 for more information on the conditions for obtaining the hydrolysates.
S1, S2, S3: semi-synthetic medium 1, 2 and 3, respectively; $t_F$: fermentation time; $G_i$: initial glucose concentration; $X_i$: initial xylose concentration; $C_G$: glucose consumption; $C_X$: xylose consumption; B: butanol; IE: isopropanol and ethanol; HAc: acetic acid; HBu: butyric acid; $\Delta X$: overall biomass growth; $Y_{B/G}$: overall sugars to butanol conversion yield; $Y_{IBE/G}$: overall sugars to IBE conversion yield; $Q_B$: overall butanol productivity; $Q_{IBE}$: overall IBE productivity
[a]Produced butanol to IBE molar ratio

A proposed process which intends to produce biofuels and/or commodity chemicals must result in products at high titers and yields to be cost-competitive. In this part of the study, both ABE and IBE fermentations allowed to obtained high overall sugars to butanol yield (0.21 g/g) at high initial sugar concentration (up to 50 g/L), even though

incomplete sugar conversion to product was obtained in IBE fermentation at this condition. However, it was reported by other authors that IBE mixture represents more attractive than ABE for biofuel application, for instance, owing to acetone corrosiveness to rubber or plastic engine parts and isopropanol higher energy density and octane number (Li et al., 2018).

### *3.5. Mass balance for the coproduction process*

Considering the BEKP composition, 61% of it was recovered in the form of fermentable sugars (70% w/w glucose and 30% w/w xylose) at relatively high concentration in the enzymatic hydrolysate after enzyme-mediated pretreatment. After the fermentation step, it was possible to completely converted these sugars into butanol and value-added coproducts (acetone or isopropanol, and ethanol). Additionally, 39.2% of BEKP was effectively extracted in the form of CNF from cellulose fibers after enzymatic hydrolysis and ball milling. Thus, for an initial 100 kg of BEKP, the proposed integrated process allows to recover 39.2 g of CNF, and 19 kg of ABE mixture (62% w/w butanol and 35% w/w acetone) or 15 kg of IBE mixture (57% w/w butanol and 40% w/w isopropanol) depending on the *Clostridium* strain used (Fig. 4). The product yields achieved in this study resulted comparable or even higher to those reported by other authors using both cellulose and hemicellulose fractions in lignocellulosic materials (Table 6). For example, Bondancia et al. (2017) used BEKP as cellulosic feedstock and reported a recovery of 37% of the initial BEKP as CNC and 39% as glucose for ethanol production. Also, Wang et al. (2021) used bleached hardwood Kraft pulp (BHKP) for CNC extraction by acid hydrolysis and reported a recovery of approximately 9% and 91% of the initial BHKP as CNC and glucose for ethanol fermentation, respectively. Both studies reached bioethanol production yields in the range of 25-34 kg of ethanol per 100 kg of cellulosic material, while this study achieved biobutanol production yields in

the range of 8.4-11.7 kg of butanol per 100 kg of BEKP. This was expected considering the higher production yields of ethanol fermentation compared to butanol fermentation.

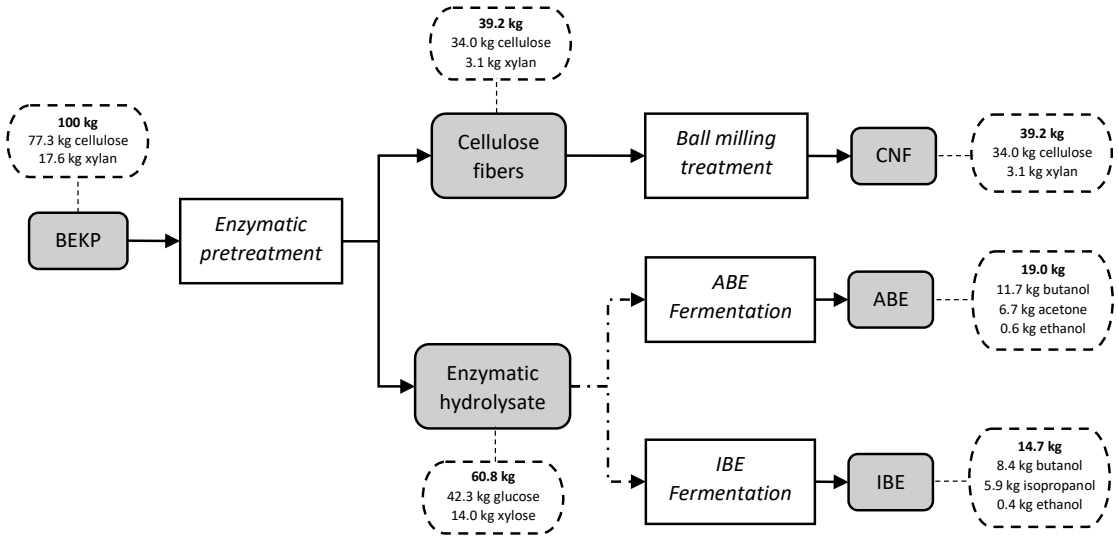


**Fig 4.** Mass balance for the proposed biobutanol and cellulose nanofibers (NFC) coproduction process from an initial dry bleached eucalyptus kraft pulp (BEKP) of 100 kg.

On the other hand, the integrated coproduction of CNM and biofuels or other chemicals were also studied using lignocellulosic materials. For instance, Pereira et al. (2021) using sugarcane bagasse reported recovery of 30% of the initial xylan as XOS, 52% of the initial lignin as lignin nanoparticles (LNP), and approximately 38% of the initial cellulose as sugars for ethanol production. Du et al. (2017) using Douglas-fir wood chips recovered 12% of the initial cellulose as CNC, 24% as glucose, and 21% of the initial xylan/mannan as xylose/mannose. This demonstrates that the coproduction strategy proposed in this study has the potential to improve productivity and enable maximal value recovery from cellulosic materials.

546 **Table 6.** Literature review of enzyme-mediated biorefinery processes that coproduce cellulose nanomaterials (CNM) and biofuels or value-added chemicals.

| Raw Material | Composition RM (wt%) | Enzyme pretreatment of cellulose-rich pulp | Pretreatment for CNM production | Overall CNM yield (wt% RM) | Overall co-products yield (wt% RM) | Microorganism for fermentation | Reference |
|---|---|---|---|---|---|---|---|
| Bleached hardwood Kraft pulp | [a]Cellulose: 79.1<br>Xylan: 21.2<br>Lignin: 4.0 | Non-commercial NS 51129 (Novozymes®) 15 FPU/g; 50°C, pH 4.8; 10% solids; 8 h | Acid hydrolysis: 64 wt% $H_2SO_4$, 45°C, 2 h | CNC: 8.9 | [b]Ethanol: 24.8 | Modified *Saccharomyces cerevisiae* Y128 | Wang et al., 2021 |
| Sugarcane bagasse | Glucan: 42.4<br>Xylan: 22.1<br>Lignin: 22.1 | Cellic CTec2 (Novozymes®) 15 mg/$g_{solid}$; 50°C; pH 4.8; 17.5% solids; 72 h | Disc ultra-refining: 1% w/w, 1600 rpm, 100 µm distance grinding discs, 1-13 cycles | CNF: 26.1 | Ethanol: 9.4<br>XOS: 6.6<br>LNP: 11.6 | *Saccharomyces cerevisiae* MH36 (Mangrove Jack) | Pereira et al., 2021 |
| Bleached eucalyptus Kraft pulp | Cellulose: 75.6<br>Hemicellulose: 14.6<br>Lignin: 6.7<br>Ash: 1.1 | Cellic CTec3 (Novozymes®) 10 mg/$g_{solid}$; 50°C; pH 5; 20% solids; 24 h | Enzymatic hydrolysis: Cellic CTec3 10 mg/$g_{solid}$; 35°C; pH 5; 20% solids; 120 h | [b]CNC: 36.9 | [b]Ethanol: 19.4 | *Saccharomyces cerevisiae* (Fleischmann) | Bondancia et al., 2017 |
| Douglas-fir wood chips | Glucan: 44.6<br>Xylan/mannan: 16.7<br>Lignin: 32.0<br>Others: 4.9 | Cellic CTec2 + Cellic HTec2 (Novozymes®) 5.5 g/100$g_{solid}$; 50°C; pH 4.8-5.3; 19% solids; 8 h | Acid hydrolysis: 64 wt% $H_2SO_4$, 44°C, 30 min | CNC: 5.6 | Glucose: 12.1<br>Xylose/Mannose: 4.0 | na | Du et al., 2017 |
| Bleached Softwood Kraft pulp | Glucan: 79.2<br>Xylan: 15.3<br>Lignin: 1.2 | *Caldicellulosiruptor bescii* DSM6725 7.5 mg/$g_{solid}$; 75°C; 1% solids; 72 h | na | CNM: 42 | Glucose: 44 | na | Yarbrough et al., 2017 |
| Bleached eucalyptus Kraft pulp | Glucan: 77.3<br>Xylan: 17.6<br>Lignin: | Cellic CTec3 + Cellic HTec2 (Novozymes®) 4.2 mg/$g_{solid}$; 50°C; pH 4.8; 10% solids; 8 h | Ball milling: 1% w/w, 20 Hz, 80$g_{balls}$/$g_{solid}$, 1.5 h | CNF: 39.2 | Butanol: 11.7<br>AE: 7.3<br><br>Butanol: 8.4<br>IE: 6.3 | *Clostridium beijerinckii* DSM 6422<br><br>*Clostridium beijerinckii* DSM 6423 | This study |

RM: raw material; CNC: cellulose nanocrystals; XOS: xylo-oligosaccharides; LNP: lignin nanoparticles; AE: acetone and ethanol; IE: isopropanol and ethanol; na: not applicable

[a]Source: Beyene et al., 2017; [b]Calculated from data reported by the authors.

547

## 4. Conclusions

Eucalyptus cellulose fibers were partially hydrolyzed by cellulase and xylanases cocktails at high solid concentrations and low enzyme loading. The enzymatic cocktail employed during enzymatic pretreatment made cellulose fibers more swollen and accessible by breaking the cellulose network, which caused fiber surface changes that influenced subsequent fiber size reduction. The by-product streams containing relatively high amount of sugars (50 g/L) were completely fermented into biobutanol and coproducts (acetone and isopropanol) using native *Clostridium beijerinckii* with a concentration close to 15 g/L. The enzymatic pretreatment of the cellulose fibers and subsequent mechanical defibrillation by ball milling allowed to obtain CNF with a width of 4-14 nm and an aspect ratio of 220-230. Differences on CNF size distribution indicated that process conditions during enzymatic pretreatment such as solid concentration and hydrolysis time influenced fiber fragmentation and/or fibrillation by ball milling through fiber structure alterations. In conclusion, the feasibility of coproducing CNF and biobutanol as high value-added products from eucalyptus pulp was demonstrated in this study. This work serves as an important starting point for future studies regarding the coproduction of biomaterials and value-added chemicals in a lignocellulosic biorefinery.

## Acknowledgments

The authors thank the Agencia Nacional de Investigación e Innovación from Uruguay (ANII_FMV_1_2019_1_156233) for providing financial support, UPM Fray Bentos (Uruguay) for providing the raw material, and Novozymes (Davis, CA) for providing the enzymes. Florencia Cebreiros thanks the Transmission Electron Microscopy Laboratory at the Electron Microscopy Unit (Facultad de Ciencias, UdelaR, Uruguay) for TEM analysis.

572 **References**

573 Bauli, C.R., Rocha, D.B., de Oliveira, S.A., Rosa, D.S., 2019. Cellulose nanostructures
574 from wood waste with low input consumption. J. Clean. Prod., 211, 408-416. DOI:
575 10.1016/j.jclepro.2018.11.099

576 Berto, G.L., Mattos, B.D., Rojas, O.J., Arantes, V., 2021. Single-step fiber pretreatment
577 with monocomponent endoglucanase: Defibrillation energy and cellulose
578 nanofibril quality. ACS Sustain. Chem. Eng., 9(5), 2260-2270. DOI:
579 10.1021/acssuschemeng.0c08162

580 Beyene, D., Chae, M., Dai, J., Danumah, C., Tosto, F., Demesa, A.G., Bressler, D.C.,
581 2017. Enzymatically-mediated co-production of cellulose nanocrystals and
582 fermentable sugars. Catalysts 7, 322. DOI: 10.3390/catal7110322

583 Birgen, C., Dürre, P., Preisig, H.A., Wentzel, A., 2019. Butanol production from
584 lignocellulosic biomass: revisiting fermentation performance indicators with
585 exploratory data analysis. Biotechnol. Biofuels, 12(1), 1-15. DOI:
586 10.1186/s13068-019-1508-6

587 Bondancia, T.J., Mattoso, L.H.C., Marconcini, J.M., Farinas, C.S., 2017. A new approach
588 to obtain cellulose nanocrystals and ethanol from eucalyptus cellulose pulp via the
589 biochemical pathway. Biotechnol. Prog., 33(4), 1085-1095. DOI:
590 10.1002/btpr.2486

591 Cao, X., Chen, Z., Liang, L., Guo, L., Jiang, Z., Tang, F., Yun, Y., Wang, Y., 2020. Co-
592 valorization of paper mill sludge and corn steep liquor for enhanced n-butanol
593 production with *Clostridium tyrobutyricum* Δcat1: adhE2. Bioresour. Technol.,
594 296, 122347. DOI: 10.1016/j.biortech.2019.122347

595 Cebreiros, F., Ferrari, M. D., Lareo, C., 2019. Cellulose hydrolysis and IBE fermentation
596 of eucalyptus sawdust for enhanced biobutanol production by *Clostridium*
597 *beijerinckii* DSM 6423. Ind. Crops Prod., 134, 50-61. DOI:
598 10.1016/j.indcrop.2019.03.059

599 Cebreiros, F., Risso, F., Cagno, M., Cabrera, M.N., Rochón, E., Jauregui, G., Boix, E.,
600 Böthig, S., Ferrari M.D., Lareo, C., 2021a. Enhanced production of butanol and
601 xylosaccharides from *Eucalyptus grandis* wood using steam explosion in a semi-
602 continuous pre-pilot reactor. Fuel, 290, 119818. DOI: 10.1016/j.fuel.2020.119818

603 Cebreiros, F., Seiler, S., Dalli, S.S., Lareo, C., Saddler, J., 2021b. Enhancing cellulose
604 nanofibrillation of eucalyptus Kraft pulp by combining enzymatic and mechanical
605 pretreatments. Cellulose, 28(1), 189-206. DOI: 10.1007/s10570-020-03531-w

606 Cesaro, A., Belgiorno, V., 2015. Combined biogas and bioethanol production:
607 opportunities and challenges for industrial application. Energies, 8, 8121-8144.
608 DOI: 10.3390/en8088121

609 Chen, Y., Wan, J., Dong, X., Ma, Y., 2013. Fiber properties of eucalyptus kraft pulp with
610 different carboxyl group contents. Cellulose, 20(6), 2839-2846. DOI:
611 10.1007/s10570-013-0055-8

612 Chen, G., Wan, J., Ma, Y., Wang, Y., 2021. Characterization of fibers after xylanase and
613 modified laccase-glutamate system biobleaching of old newsprint pulp. Nord.
614 Pulp Pap. Res. J., 36(1), 21-32. DOI: 10.1515/npprj-2020-0089

615 Cho, E. J., Trinh, L. T. P., Song, Y., Lee, Y. G., Bae, H. J., 2020. Bioconversion of
616 biomass waste into high value chemicals. Bioresour. Technol., 298, 122386. DOI:
617 10.1016/j.biortech.2019.122386

618 da Silva, A.S.A., Espinheira, R.P., Teixeira, R.S.S., de Souza, M.F., Ferreira-Leitão, V.,
619 Bon, E.P., 2020. Constraints and advances in high-solids enzymatic hydrolysis of
620 lignocellulosic biomass: a critical review. Biotechnol. Biofuels, 13(1), 1-28. DOI:
621 10.1186/s13068-020-01697-w

622 dos Santos Vieira, C.F., Codogno, M.C., Maugeri Filho, F., Maciel Filho, R., Mariano,
623 A.P., 2021. Sugarcane bagasse hydrolysates as feedstock to produce the
624 isopropanol-butanol-ethanol fuel mixture: Effect of lactic acid derived from
625 microbial contamination on *Clostridium beijerinckii* DSM 6423. Bioresour.
626 Technol., 319, 124140. DOI: 10.1016/j.biortech.2020.124140

627 Du, L., Wang, J., Zhang, Y., Qi, C., Wolcott, M.P., Yu, Z., 2017. A co-production of
628 sugars, lignosulfonates, cellulose, and cellulose nanocrystals from ball-milled
629 woods. Bioresour. Technol., 238, 254-262. DOI: 10.1016/j.biortech.2017.03.097

630 Engström, A.C., Ek, M., Henriksson, G., 2006. Improved accessibility and reactivity of
631 dissolving pulp for the viscose process: pretreatment with monocomponent
632 endoglucanase. Biomacromolecules, 7(6), 2027-2031. DOI: 10.1021/bm0509725

633 Espinosa, E., Rol, F., Bras, J., Rodríguez, A., 2019. Production of lignocellulose
634 nanofibers from wheat straw by different fibrillation methods. Comparison of its
635 viability in cardboard recycling process. J. Clean. Prod., 239, 118083. DOI:
636 10.1016/j.jclepro.2019.118083

637 Foster, E.J., Moon, R.J., Agarwal, U.P., Bortner, M.J., Bras, J., Camarero-Espinosa, S.,
638 Chan, K.J., Clift, M.J.D., Cranston, E.D., Eichhonr, S.J., Fox, D.M., Hamad,
639 W.Y., Heux, L., Jean, B., Korey, M., Nieh, W., Ong, K.J., Reid, M.S., Renneckar,
640 S., Roberts, R., Shatkin, J.A., Simonsen, J., Stinson-Bagby, K., Wanasekara, N.,

Youngblood, J., 2018. Current characterization methods for cellulose nanomaterials. Chem. Soc. Rev., 47:2511–3006. DOI: 10.1039/C6CS00895J

Gourlay, K., Van Der Zwan, T., Shourav, M., Saddler, J., 2018. The potential of endoglucanases to rapidly and specifically enhance the rheological properties of micro/nanofibrillated cellulose. Cellulose, 25(2), 977-986. DOI: 10.1007/s10570-017-1637-7

Gu, F., Wang, W., Cai, Z., Xue, F., Jin, Y., Zhu, J.Y., 2018. Water retention value for characterizing fibrillation degree of cellulosic fibers at micro and nanometer scales. Cellulose, 25(5), 2861-2871. DOI: 10.1007/s10570-018-1765-8

Katz, S., Beatson, R.P., 1984. The determination of strong and weak acidic groups in sulfite pulps. Sven Papperstidn. 87:48–53.

Li, Y., Chen, Y., Wu, G., Lee, C. F., Liu, J., 2018. Experimental comparison of acetone-n-butanol-ethanol (ABE) and isopropanol-n-butanol-ethanol (IBE) as fuel candidate in spark-ignition engine. Appl. Therm. Eng., 133, 179–187. DOI: 10.1016/j.applthermaleng.2017.12.132

Lou, L., Osemwegie, O., Ramkumar, S.S., 2020. Functional nanofibers and their applications. Ind. Eng. Chem. Res., 59(13), 5439-5455. DOI: 10.1021/acs.iecr.9b07066

Martinez, D., Buckley, K., Jivan, S., Lindstrom, A., Thiruvengadaswamy, R., Olson, J., Ruth, T., Kerekes, R., 2001. Characterizing the mobility of papermaking fibres during sedimentation, in: Baker, C.F. (Ed.), The Science of Papermaking, Transactions of the 12th Fundamental Research Symposium. The Pulp and Paper Fundamental Research Society, Bury, Lancaster, UK, pp. 225–254. DOI: 10.15376/frc.2001.1.225

Meng, X., Yoo, C.G., Li, M., Ragauskas, A.J., 2016. Physicochemical structural changes of cellulosic substrates during enzymatic saccharification. J. Appl. Biotechnol. Bioeng., 1(3), 87-94. DOI: 10.15406/jabb.2016.01.00015

Michelin, M., Gomes, D. G., Romaní, A., Polizeli, M.D.L., Teixeira, J.A., 2020. Nanocellulose production: exploring the enzymatic route and residues of pulp and paper industry. Molecules, 25(15), 3411. DOI: 10.3390/molecules25153411

Moser, C., Lindström, M.E., Henriksson, G., 2015. Toward industrially feasible methods for following the process of manufacturing cellulose nanofibers. BioResources, 10(2), 2360-2375. DOI: 10.15376/biores.10.2.2360-2375

Pereira, B., Arantes, V., 2020. Production of cellulose nanocrystals integrated into a biochemical sugar platform process via enzymatic hydrolysis at high solid loading. Ind. Crops Prod., 152, 112377. DOI: 10.1016/j.indcrop.2020.112377

Pereira, B., Marcondes, W.F., Carvalho, W., Arantes, V., 2021. High yield biorefinery products from sugarcane bagasse: Prebiotic xylooligosaccharides, cellulosic ethanol, cellulose nanofibrils and lignin nanoparticles. Bioresour. Technol., 342, 125970. DOI: 10.1016/j.biortech.2021.125970

Raj, P., Mayahi, A., Lahtinen, P., Varanasi, S., Garnier, G., Martin, D., Batchelor, W., 2016. Gel point as a measure of cellulose nanofibre quality and feedstock development with mechanical energy. Cellulose, 23(5), 3051-3064. DOI: 10.1007/s10570-016-1039-2

Ramos, L.P., Nazhad, M.M., Saddler, J.N., 1993. Effect of enzymatic hydrolysis on the morphology and fine structure of pretreated cellulosic residues. Enzyme Microb. Technol., 15(10), 821–831. DOI: 10.1016/0141-0229(93)90093-H

688 Sanchez-Salvador, J.L., Campano, C., Lopez-Exposito, P., Tarrés, Q., Mutjé, P.,
689 Delgado-Aguilar, M., Monte, M.C., Blanco, A., 2021. Enhanced Morphological
690 Characterization of Cellulose Nano/Microfibers through Image Skeleton
691 Analysis. Nanomater., 11(8), 2077. DOI: 10.3390/nano11082077

692 Segal, L., Creely, J.J., Martin, A.E., Conrad, C.M., 1959. An empirical method for
693 estimating the degree of crystallinity of native cellulose using the X-ray
694 diffractometer. Text Res. J. 29:786–794. DOI: 10.1177/004051755902901003

695 Siqueira, G.A., Dias, I.K., Arantes, V., 2019. Exploring the action of endoglucanases on
696 bleached eucalyptus kraft pulp as potential catalyst for isolation of cellulose
697 nanocrystals. Int. J. Biol. Macromol., 133, 1249-1259. DOI:
698 10.1016/j.ijbiomac.2019.04.162

699 Squinca, P., Bilatto, S., Badino, A.C., Farinas, C.S., 2020. Nanocellulose production in
700 future biorefineries: An integrated approach using tailor-made enzymes. ACS
701 Sustain. Chem. Eng., 8(5), 2277-2286. DOI: 10.1021/acssuschemeng.9b06790

702 Varanasi, S., He, R., Batchelor, W., 2013. Estimation of cellulose nanofibre aspect ratio
703 from measurements of fibre suspension gel point. Cellulose, 20, 1885–1896. DOI:
704 10.1007/s10570-013-9972-9

705 Veza, I., Said, M.F.M., Latiff, Z.A., 2021. Recent advances in butanol production by
706 acetone-butanol-ethanol (ABE) fermentation. Biomass Bioenerg., 144, 105919.
707 DOI: 10.1016/j.biombioe.2020.105919

708 Wang, J., Chae, M., Beyene, D., Sauvageau, D., Bressler, D.C., 2021. Co-production of
709 ethanol and cellulose nanocrystals through self-cycling fermentation of wood pulp
710 hydrolysate. Bioresour. Technol. 330, 124969. DOI:
711 10.1016/j.biortech.2021.124969

712 Yarbrough, J.M., Zhang, R., Mittal, A., Vander Wall, T., Bomble, Y.J., Decker, S.R.,
713 Himmel, M.E., Ciesielski, P.N., 2017. Multifunctional cellulolytic enzymes
714 outperform processive fungal cellulases for coproduction of nanocellulose and
715 biofuels. ACS Nano, 11(3), 3101-3109. DOI: 10.1021/acsnano.7b00086

716 Zhou, Y.M., Fu, S.Y., Zheng, L.M., Zhan, H.Y., 2012. Effect of nanocellulose isolation
717 techniques on the formation of reinforced poly (vinyl alcohol) nanocomposite
718 films. Express Polym. Lett., 6(10):794-804. DOI:
719 10.3144/expresspolymlett.2012.85